Drug Design, Development and Therapy

Dovepress
Taylor & Francis Group

Open Access Full Text Article

ORIGINAL RESEARCH

Recombinant Hydrophobic Polypeptide MBAY Loaded Into SPION-Exosome Realizes Sustained-Release to Improve Type 2 Diabetes Mellitus

Xinyu Zong[1,2,*], Shangying Xiao[3,*], Haishan Xia[3], Dan Guo[1], Jiaping Wu[1], Manjiao Zhuang[3], Lei Rao[1]

[1]Guangdong Provincial Key Laboratory of Utilization and Conservation of Food and Medicinal Resources in Northern Region, Medical College, Shaoguan University, Shaoguan, 512005, People's Republic of China; [2]School of Pharmacy, Anhui Medical University, Hefei, Anhui, 230032, People's Republic of China; [3]School of Pharmacy, Guangdong Medical University, Dongguan, Guangdong, 523808, People's Republic of China

*These authors contributed equally to this work

Correspondence: Lei Rao, Guangdong Provincial Key Laboratory of Utilization and Conservation of Food and Medicinal Resources in Northern Region, Medical college, Shaoguan University, Shaoguan, 512005, People's Republic of China, Email 591617735@qq.com; Manjiao Zhuang, School of Pharmacy, Guangdong Medical University, Dongguan, Guangdong, 523808, People's Republic of China, Email man.jiao@163.com

Background: BAY55-9837, a potential therapeutic peptide for the treatment of type 2 diabetes mellitus (T2DM), can induce glucose (GLC)-dependent insulin secretion. Our previous study has demonstrated that the use of superparamagnetic iron oxide nanoparticle-decorated exosome (exosome-SPION) and external magnetic force (MF) enables BAY 55-9837 to target pancreatic islets. However, the initial burst release of BAY 55-9837 loaded within exosome-SPION shortens its in vivo half-life and consequently reduces the frequency of GLC responsiveness. Therefore, in our study, the transmembrane hydrophobic structure of the exosome signature protein CD81 was fused with BAY 55-9837 to obtain MBAY with sustained-release capability.

Methods: MBAY was fabricated via genetic engineering, and the dissociation constant (Kd) was determined to assess its affinity for vasoactive intestinal peptide receptor type 2 (VPACII). Subsequently, MABY was incorporated into exosomes through electroporation to obtain MBAY-exosome, and SPOIN was adorned on MBAY-exosome by means of the self-assembly of transferrin (Tf) and the transferrin receptor (TfR). The in vitro release profile and in vivo pharmacokinetic profile of MBAY-Exosome-SPION were detected using high-performance liquid chromatography (HPLC). The L9(3^4) orthogonal design approach was utilized to optimize the drug administration mode in vivo. The therapeutic effect of MBAY-exosome-SPIONs/MF on T2DM was assessed both in vitro and in vivo.

Results: In vitro studies showed that the release rate of MBAY from exosome-SPION was slower compared with BAY 55-9837. Meanwhile, MBAY still maintained high affinity and selectivity for VPAC II and MBAY-exosome-SPIONs/MF could effectively promote insulin secretion in response to elevated GLC as BAY-exosome-SPIONs/MF. In vivo studies indicated that MBAY-exosome-SPIONs had a prolonged half-life and improved pharmacokinetic parameters compared to BAY-exosome-SPIONs, which further alleviated the symptoms of T2DM model mice.

Conclusion: Thus, the reconstructed MBAY loaded in SPION-exosome realized sustained-release and exosomes-SPIONS achieved pancreatic targeting which led to ideal therapeutic effect in T2DM mice.

Keywords: type 2 diabetes mellitus, exosome, BAY 55-9837, sustained-release

Introduction

Diabetes is a chronic disorder that poses a significant threat to human health. Type 2 diabetes mellitus (T2DM) is the most common form of diabetes, making up about 90% of all diabetes cases.[1] The primary goal in the treatment of T2DM is to achieve effective Blood Glucose (GLC) control. Chronically elevated blood GLC levels not only reduce the patient's

Received: 29 October 2024
Accepted: 12 March 2025
Published: 22 April 2025

ability to regulate blood GLC but also cause the development and worsening of various complications.[2] Controlling blood GLC relies on the accurate regulation of insulin secretion. In normal physiological situations, insulin secretion rises along with increasing blood GLC levels.[3,4] Insulin and insulin secretagogues are prevalently utilized approaches for blood GLC management, yet the majority of medications still suffer from the drawback of inferior blood GLC responsiveness.[5]

Currently, the newly developed insulin drugs are mainly combination formulations designed to achieve blood glucose responsiveness. For example, Insulin Degludec/Insulin Aspart combines different stable insulins into a blended formulation. It consists of 70% basal insulin (Degludec) and 30% mealtime insulin (Aspart).[6] Basal insulin can provide a long-acting insulin function, while mealtime insulin can rapidly reduce blood glucose after meals. However, this combination can only achieve one blood glucose response, resulting in limited treatment efficacy.[7] In addition, the commonly used insulin secretagogues, such as sulfonylureas and gliptins, have a strong effect in stimulating insulin secretion. Nevertheless, they cannot respond to changes in blood GLC levels.[8,9] Meanwhile, they have significant side effects, such as liver and kidney damage, cardiovascular problems, and gastrointestinal disorders.[10]

Peptide-based insulin secretagogues have specific targets, and potent activity, thus making them potential substitutes for traditional drugs.[11] BAY 55-9837, a derivative peptide of pituitary adenylate cyclase-activating polypeptide and vasoactive intestinal peptide, exhibits GLC-dependent insulin secretion and shows great potential as a peptide drug for T2DM.[12] Nevertheless, limitations such as a short half-life and the lack of tissue targeting impede its clinical application.[13] The advancements in biotechnology and nanotechnology have resulted in significant progress in the application of nanomedicine to gene engineering drugs for the treatment of diabetes. Typically, the employment of nanoparticles enhances the bioavailability and physicochemical stability of the loaded medicine.[14]

Exosomes, serving as ideal peptide carriers, possess advantages such as non-toxicity, low immunogenicity, high tolerability, and biodegradability.[15] However, Exosomes are typically found to accumulate in the liver and subsequently in the lungs.[16] They lack a dependable targeting capability and cannot reach the pancreatic islets for targeted delivery in vivo. Achieving controllable pancreatic targeting, whereby the drug accumulates in the pancreas in a controlled manner as blood GLC levels rise, constitutes an effective strategy for fulfilling GLC responsiveness. Numerous studies have shown that exosomes can effectively target diseased tissues by coupling with targeting ligands.[17–19] Superparamagnetism, a vital feature of SPIONs, can be defined as follows: When an external magnetic force (MF) is applied, SPIONs are magnetized to their saturation magnetization. When the MF is removed, SPIONs no longer show any remaining magnetic interaction, thus giving them excellent dispersibility and targeting ability.[20] Chitosan features ideal properties, such as low toxicity and biocompatibility, thereby making it attractive for biological applications.[21] Our previous research disclosed that the chitosan-SPION decorated exosome loaded with BAY 55-9837 accomplished targeted delivery to the pancreas with the assistance of an external magnetic field (MF), enabling controlled drug accumulation and synchronous insulin secretion along with the elevation of blood GLC, thereby effectively responding to changes in blood GLC levels and exerting optimal hypoglycemic effects.[17] Nevertheless, the initial burst release of exosome-SPION affected the in vivo half-life of BAY 55-9837 and consequently decreased the frequency of GLC responsiveness. Severe initial burst release of exosomes precludes it from being an ideal drug carrier,[17,18] reducing the leakage rate of exosomes is of crucial importance for further enhancing the GLC responsiveness of BAY 55-9837.

Extensive research has been conducted on sustained-release technologies for reducing the release rate of polypeptide drugs. Due to the fluidity of exosome structures at body temperature, the release pores cannot be regulated.[15] BAY 55-9837 is a polypeptide which can enhance its hydrophobicity via genetic engineering to function as a blocker, thereby attaining sustained release when loaded into an exosome constituted by a lipid bilayer. The transmembrane structure of the exosomal marker protein CD81 encompasses an α-helical hydrophobic peptide segment with a distinct sequence and structure,[22,23] and this can be exploited to construct fusion proteins to increase the hydrophobicity of BAY 55-9837.

In this paper, the transmembrane structure of the exosome signature protein CD81 was fused with BAY 55-9837 via genetic engineering technology to construct MBAY with enhanced hydrophobicity. Subsequently, MBAY was loaded into exosome-SPION. By utilizing SPION/MF, MBAY was endowed with magnetic targeting capacity, aiming to achieve the multiple controllable magnetic targeting delivery of secretagogue drugs in pancreatic tissue and hoping to simulate the normal insulin secretion pattern. The enhanced hydrophobicity of MBAY led to an initial burst release when it was

loaded into SPION-exosome, thereby fulfilling the purpose of sustained release and further obtaining the long-term effect of multiple blood GLC responses in the treatment of T2DM.

Material and Methods

Materials

Tetramethylbenzidine, SA-HRP, L-glutamine, HEPES, 2-mercaptoethanol and Streptozocin were obtained from Aladdin (Shanghai, China). DMEM medium and fetal bovine serum were purchased from Gibco (Gaithersburg, MD, USA). Penicillin and streptomycin were procured from Invitrogen (CA, USA), and β-mercaptoethanol was purchased from Gibco (Gaithersburg, MD, USA). Mouse insulin ELISA kit was purchased from MEIMIAN (Jiangsu, China). Fluo-3 AM was purchased from Solarbio (Wuhan, China). Mouse cAMP ELISA kit was purchased from FineTest (Wuhan, China).

Preparation and Identification of the Recombinant MBAY

Recombinant expression vectors, namely pTXB1-MBAY F1, pTXB1-MBAY F2, pTXB1-MBAY F3, and pTXB1-MBAY F4, were transfected into E. coli ER2566. Then, they were induced for expression with IPTG. After purifying the cell lysate via chitin beads affinity chromatography, the recombinant MBAY was further refined and prepared by means of a reverse-phase high-performance liquid chromatography (HPLC) system equipped with a 9.4×250 mm, 5 um, ZORBAX SB-C18 column (Agilent Technologies, Beijing, China). The purification procedure entailed a gradient elution of acetonitrile ranging from 5% to 70% within 35 minutes at a flow rate of 1 mL/min. Subsequently, the purified recombinant MBAY was dried by lyophilization. The identity of the recombinant MBAY was confirmed by electrospray ionization mass spectrometry (ESI-MS; Applied Biosystems, Foster City, USA), and its purity was evaluated using HPLC analysis.

Evaluation of the Binding Ability of MABY to Different Receptors

The binding affinity of MBAY to PAC1, vasoactive intestinal peptide receptor type 1 (VPAC I) and VPAC II was analyzed using ELISA.[24] Enzyme immunoassay plates were coated with 100 μL of 1 nmol/L, 2.5 nmol/L, 5 nmol/L, 10 nmol/L, 50 nmol/L, 100 nmol/L, 200 nmol/L, 500 nmol/L and 1000 nmol/L PAC I,VPAC I and VPAC II, respectively, and then stored at 4 °C overnight. Thereafter, wells were washed three times with PBST (10 mm PBS, 0.05% Tween-20, pH 7.4,). The plate was blocked with 300 μL per well of 1% BSA (10 mm PBS, pH 7.4) for 2 h at 37 °C and then washed three times with PBST again. 10 pmol of biotin-labelled MBAY was added and incubated for 1 h at 37 °C. Subsequently, the plate was washed again, 100 μL of secondary detector solution SA-HRP at a dilution of 1/8,000 in PBS was added and the plate was incubated for 1 h at 37 °C. The plate was again washed five times and 100 μL of tetramethylbenzidine (TMB) chromogenic solution was added and incubated for 25 min at 37 °C. The reaction was stopped by adding 100 μL of 2 M H_2SO_4, and the absorbance of the resulting solution was read at 450 nm using a microtiter plate reader (Molecular Devices, Sunnyvale, CA, USA). The dissociation constant (Kd) between MBAY and VPACII was quantified by Originpro 2021 software.

Synthesis of the MBAY-Exosome-SPIONs

Chitosan decorated SPIONs (CS-SPIONs) were fabricated and collected as in our previous research,[17] with a carboxylated CS concentration of 0.08 mg/mL. 200 μL of CS-SPIONs (1 mg/mL) were mixed with carbodiimide (EDC) and NHS at a molar ratio of 1:2:3, and then the mixture was incubated at 37 °C for 1 h (pH 5.5). To stop the reaction, 5 μL of 2-mercaptoethanol was added to the mixture. The CS-SPIONs with an activated carboxylic group were obtained through magnetic separation and then re-suspended in the same volume of phosphate buffered saline (PBS, pH 7.4). Subsequently, 10 μg of Tf was incubated with the activated CS-SPIONs for 12 h at 4 °C. Then, Tf-SPIONs were harvested through magnetic separation and re-suspended in PBS after three washes. The Tf-SPIONs were stored at 4 °C.

Human mesenchymal stem cell (HuMSC)-derived exosomes were harvested according to a previous study.[18] Briefly, huMSCs (3×10^6 cells/well) were cultured in a 10-cm dish for 24 h, followed by transferring the cell culture supernatant into a dialysis bag and dialyzing it against PBS for 24 h. Subsequently, the dialyzed supernatant was centrifuged to

remove the cells (at 200 × g for 5 minutes). The collected supernatant was successively centrifuged (at 12,000 × g for 45 minutes) and filtered through a 0.22 μm filter membrane to further reduce cell debris. For MBAY loading, 50 μL of the MBAY solution (1 mg/mL) was added to the exosome solution (150 μL, 1 mg/mL) with gentle agitation. After electroporation at 350 V and 150 ms in 0.4-cm electroporation cuvettes using an Electroporator (Bio-Rad, USA), the mixture was incubated at 37 °C for 30 minutes to ensure the complete restoration of the plasma membrane of the exosomes, thereby generating MBAY-exosomes. 2 mL of the MBAY-exosome was dialyzed against PBS for 12 h.

Thereafter, the MBAY-exosome was mixed with 200 μL of the Tf-SPION solution (0.5 mg/mL) and incubated for 8 h at 4 °C. The MBAY-exosome-SPION was obtained after magnetic separation and washed three times with PBS. The MBAY-exosome-SPION was stored at 4 °C before being used.

Characterization of MBAY-Exosome-SPION

To assess the surface morphology of MBAY-exosome-SPION, it was re-dispersed in 200 μL of distilled water and the solution gently shaken for 10 minutes. The morphology of MBAY-exosome-SPION was characterized using a high-resolution TEM (JSM-7500F, JEOL Ltd., Japan). To measure the size distribution, a Zetasizer Nano (Malvern Instruments, Malvern, UK) was used. To evaluate the stability of MBAY-exosome-SPION at specific intervals, its particle size was determined using a Zetasizer Nano. Additionally, the concentration of MBAY was measured by HPLC.

Release Profile of MAY-Exosome-SPION

The release profile of MBAY was detected by a procedure according to previous reports.[17] MBAY-exosome-SPION was placed in a dialysis bag (molecular weight cut off: 80 kD) for incubation at 37 °C in PBS. At selected time intervals, using a pipette, samples were removed from the vial and the amount of MBAY was detected. Then, an equation to evaluate the release rate is as follows: An equation for evaluating the release rate is as follows: Percentage = (MBAY concentration in PBS × PBS volume) / (MBAY concentration in mother liquors × mother liquors volume) × 100 %.

High Performance Liquid Chromatography Analysis of MBAY

The concentration of MBAY was determined in accordance with the established HPLC method as described in our previous study.[25] Briefly, HPLC analysis was performed on a Waters Alliance 2695–2487 hPLC system equipped with an Agilent C18 column (Agilent, USA). The components were eluted via a gradient elution at a flow rate of 1 mL/min. Chromatography was performed at 40°C. The mobile phase A was H_2O (with 0.1% TFA), and the mobile phase B was CH_3CN (with 0.1% TFA). The effluent was detected at 280 nm, and subsequently, the raw data were analyzed using Empower software.

Cell Culture

The insulin-secreting cell line MIN-6 was obtained from the Cell Bank of the Chinese Academy of Sciences (Beijing, China) and cultured in DMEM that was supplemented with 10% fetal bovine serum, 100 U/mL penicillin, 100 mg/mL streptomycin, 2 mmol/L L-glutamine, 10 mmol/L HEPES (4-(2-hydroxyethyl)-1-piperazineethanesulfonic acid), 1 mmol/L sodium pyruvate, and 50 mmol/L 2-mercaptoethanol within a humidified atmosphere (5% CO_2, 37 °C).[26] Cells were seeded in 96-well plates (1×10^4 cells/well) for viability assays or insulin secretion.

Measurement of Cell Activity, Insulin Secretion and Signal Pathway Detection

The activity of MIN-6 cells was determined using 3-(4,5-dimethyl-2-thiazolyl)-2,5-diphenyl-2-H-tetrazolium bromide (MTT). Cells were seeded in 96-well plates until reaching 70% confluence. Subsequently, the cells were incubated with BAY 55-9837, MBAY F1, MBAY F2, MBAY F3, and MBAY F4 (ranging from 0.1 to 100 nmol/L) for 24 h. Then, the cells were further incubated with 0.5 mg/mL of MTT (3-(4,5-dimethylthiazol-2-yl)-2,5-diphenyl tetrazolium bromide) for an additional 4 h in the dark within a humidified atmosphere (5% CO_2, 37 °C). Thereafter, the cells were washed with PBS, and the precipitates were dissolved in 100 μL of dimethyl sulfoxide. The absorbance of the reduced intracellular formazan product was measured at 490 nm using a microtiter plate reader (Molecular Devices, Sunnyvale, CA, USA).

For the insulin secretion studies, 1×105 min-6 cells were plated in a 6-well microplate and cultured for 48 h. Then, the medium in each well was removed, and 1 mL of fresh medium was added. 100 nmol/L of BAY 55-9837, BAY-exosome-SPION/MF (MF density: 1 T), and MBAY-exosome-SPION/MF (MF density: 1 T) were incubated with MIN-6 cells for 1 h. Subsequently, the medium was collected for insulin detection. The insulin concentration in the medium was determined by a commercial mouse insulin ELISA (enzyme-linked immunosorbent assay) kit in accordance with the manufacturer's instructions. Additionally, MIN-6 cells that were incubated with MBAY-exosome-SPION/MF (MF density: 1 T) for 1 h were collected for signal pathway detection. The cAMP content was detected by the ELISA kit in accordance with the manufacturer's instructions, and the intracellular Ca^{2+} probe Fluo-3 AM was employed to explore the Ca^{2+} level of MIN-6 cells.

Pharmacokinetic Studies

All animal study protocols were conducted strictly in accordance with the regulations of the Bioethics Committee of Guangdong Medical University (Approval No. GDY2002062), and the procedures were carried out in accordance with the Chinese Laboratory Animal - Guideline for Ethical Review of Animal Welfare. Kunming mice (10 weeks old, weighing 18–22 g) were randomly divided into three groups, with six mice in each group. In Group-I, BAY55-9837 was administered at a dosage of 5 mg/kg via tail vein injection. In Group-II, BAY-exosome-SPION was administered at the same dosage of BAY 55-9837 as in Group-I. In Group-III, MBAY-exosome-SPION was also administered at the same dosage of BAY 55-9837 as in Group-I. At different time intervals after injection, 20 μL blood samples were collected from the tail vein using heparinized micropipettes and quickly mixed with 1 mL of PBS. The samples were then centrifuged at 10,000 rpm for 10 minutes to obtain the supernatants. Subsequently, the concentration of BAY 55-9837 or MBAY was determined according to the established HPLC method.

Establishment of T2DM Model Mice

The C57BL/6J mice were bought from the Guangdong Medical Experimental Center and were induced with a high-fat diet and streptozocin (STZ) to create T2DM model mice. Briefly, male C57BL/6J mice were fed a high-fat diet (HFD: 59% fat, 15% protein, and 20% carbohydrates) for 12 weeks. Then, the mice were intraperitoneally injected with a low dose of STZ (30 mg/kg) for 7 days to build a T2DM mouse model. The C57BL/6J mice in the normal control group were provided with a standard diet for 12 weeks and were intraperitoneally injected with citrate-phosphate buffer. The T2DM model mice were successfully created when the random blood GLC level was over 16.7 mmol/L.[27]

Chronic Effects of MBAY-Exosome-SPION on the GLC and Lipid Profile in T2DM Mice

The mice were randomly divided into five groups, with six mice in each group. Group 1: Normal mice received an intravenous injection of 0.4 mL of saline daily for 8 weeks. Group 2: db/db mice were given an intravenous infusion of 0.4 mL of saline per day for 8 weeks. Group 3: db/db mice were administered BAY 55-9837 (5 mg/kg) intravenously each day for 8 weeks. Group 4: Mice were injected with BAY - exosome - SPION (5 mg of BAY - equiv/kg body weight) intravenously every day. Additionally, a magnet was placed over the surface of the pancreatic islets using Steri - Strip tape for 1 hour twice a day for 8 weeks.Group 5: db/db mice were injected with MBAY - exosome - SPION (5 mg of BAY - equiv/kg body weight) intravenously every day. Similarly, a magnet was positioned over the surface of the pancreatic islets using Steri - Strip tape for 1 hour twice a day for 8 weeks. After an 8 - week treatment period, the body weight, glycosylated hemoglobin, liver glycogen, and lipid profiles including blood triglycerides (TG) and hepatic TG were quantified. Glycosylated hemoglobin was determined using a Mouse Carboxy - Methyl Lysine - Advanced Glycation End Products (CML - AGE) ELISA Kit (BMASSAY, Beijing, China). The TG level was measured using a Triglyceride Quantification Assay Kit (Abcam) in accordance with the manufacturer's instructions. We used a Glycogen Content Assay Kit (Boxbio, Beijing, China) to detect the hepatic glycogen level.

Statistical Analysis

All experiments were carried out with at least 6 replicates, and the results were presented as the mean ± standard deviation. Statistical differences were evaluated by one-way analysis of variance. Unpaired two-tailed t-tests and paired two-tailed t-tests were used. They were employed to determine the statistical significance between test groups as appropriate. A p-value less than 0.05 was regarded as statistically significant (*), meaning that the results are likely not due to chance. While a p-value less than 0.01 was considered statistically highly significant (**), indicating stronger evidence of a real effect. Multiple group comparisons are performed using Tukey's test and a 95% confidence interval to determine significance.

Results

Design and Activity Analysis of the Fusion Polypeptide MBAY

CD81 protein, a biomarker of exosome, contains four α-helices.[16,23] Therefore, the CD81 sequence was chosen to be fused with the BAY 55-9837 protein sequence with the aim of obtaining recombinant proteins containing different numbers of alpha helix sequences. At the same time, in order to reduce the interaction between proteins, a flexible peptide sequence was added as the connecting sequence between BAY 55-9837 and CD81. Figure 1A shows the schematic diagram of how the fusion protein design and the added sequence of alpha helix. MBYA F1, MBYA F2, MBYA F3, and MBYA F4 are the recombinant proteins fused with one alpha helix, two alpha helices, three alpha helices, and four alpha helices, respectively. Subsequently, in order to verify whether the insulin-promoting secretion ability of

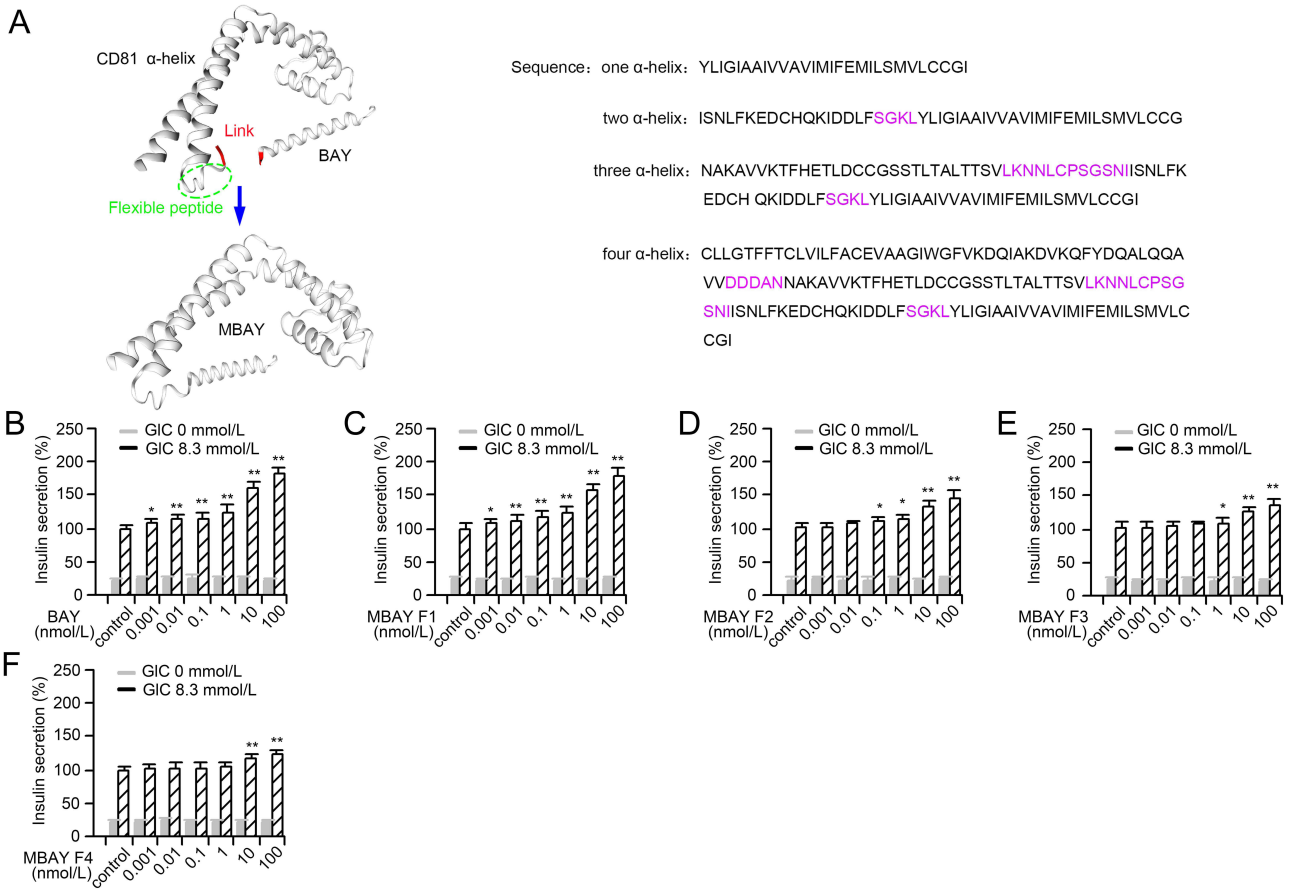

Figure 1 Design and activity analysis of the fusion polypeptide MBAY. (**A**) Schematic diagram of how the fusion protein MBAY design. A flexible peptide sequence was employed as the linkage between BAY 55-9837 and α - helix to build MBAY; The pink text indicates the turn structure; (**B**) The insulin-secreting promoting activity of BAY 55-9837; (**C**) The insulin-secreting promoting activity of MBAY F1; (**D**) The insulin-secreting promoting activity of MBAY F2; (**E**) The insulin-secreting promoting activity of MBAY F3; (**F**) The insulin-secreting promoting activity of MBAY F4. The insulin concentration in the cell culture medium was detected by mouse insulin ELISA in the presence or absence of CLC. n = 6, significance levels are shown as *$p < 0.05$ and **$p < 0.01$ vs 0 control.

 https://doi.org/10.2147/DDDT.S499641

the recombinant proteins has changed, the insulin-promoting secretion ability of BAY 55-9837, MBYA F1, MBYA F2, MBYA F3, and MBYA F4 was detected. The findings demonstrated that MBYA F1 fused with one alpha helix maintained the same insulin-promoting secretion capacity as BAY 55-9837. It could significantly promote insulin secretion at 0.01 nmol/L in a GLC-dependent manner. However, the insulin-promoting secretion capacity of the recombinant proteins fused with two to four alpha helices was lower than that of the BAY 55-9837 group. Moreover, the more alpha helices were fused, the weaker the insulin-promoting secretion ability (Figure 1B–F). As a result, MBYA F1 was chosen for the subsequent experiments.

Characterization of MBAY-Exosome-SPION

Via electroporation, MBAY was successfully incorporated into exosome-SPION, thereby obtaining MBAY-exosome-SPION. As depicted in Figure 2A and B, the average particle size of MBAY-exosome-SPION was determined to be 78.8 nm in distilled water and 92 nm in DMEM culture medium, indicating its ideal stability. The TEM image revealed that MBAY-exosome-SPION was uniform and exhibited excellent dispersibility; concomitantly, a few black spots were distributed on the surface of the exosome, further suggesting that the exosome was successfully adorned with SPIONs (Figure 2C). The modification of SPIONs bestowed MBAY-exosome-SPION with magnetic responsive properties.

Then, the stability of MBAY-exosome-SPIONs was investigated by evaluating their diameter and concentration of MBAY. As shown in Figure 2D, the diameter of the MBAY-exosome-SPIONs remained stable for 25 days, providing support for future medical applications. Additionally, the MBAY concentration was evaluated for 30 days in distilled water. As depicted in Figure 2E, MBAY was detected for up to 30 days after being loaded into exosome-SPIONs. This result occurred because the lipid bilayer of exosomes can act as a barrier to protect MBAY from degradation.

In Vitro Release Profile of MBAY-Exosome-SPION

The concentration of MBAY was determined via the established HPLC method. The HPLC method was successfully constructed with the retention time of MBAY and internal standard peptide were 14.5 min and 10.2 min (Figure 3A), respectively. Figure 3C indicated that the release rate of MBAY was slower compared with BAY 55-9837, with merely approximately 50% being released at the 60th h, while in the BAY 55-9837 group around 50% is released at the 5th

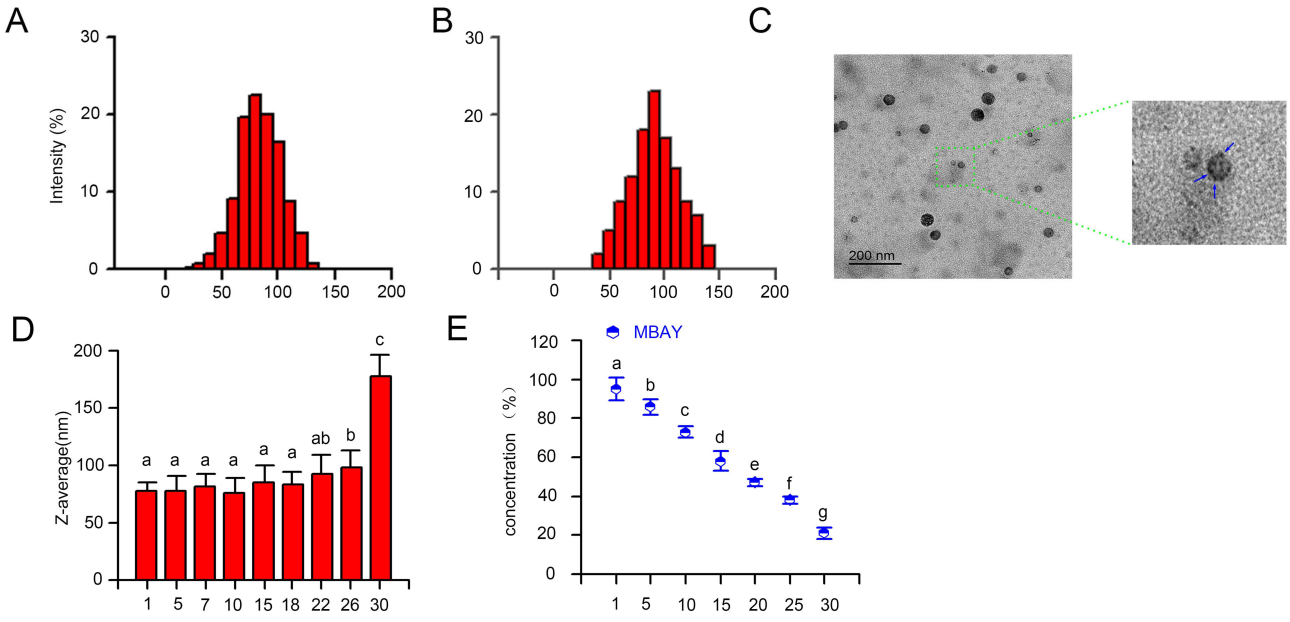

Figure 2 Characterization and identification of MBAY-exosome-SPION. The particle size distribution of MBAY-exosome-SPION in (**A**) distilled water and (**B**) DMEM culture medium was detected by a Zetasizer Nano. (**C**) The TEM image of MBAY-exosome-SPION. The blue arrows indicate the SPIONs distributed on the surface of the exosomes. (**D**) The change in the size distribution of MBAY-exosome-SPION over 30 days. (**E**) The concentration-time profile of MBAY-exosome-SPION over 30 days in terms of its concentration changes was detected by HPLC. Multiple comparison analysis of data was performed for each experimental condition. Bars with the same letter do not differ significantly. n = 6.

https://doi.org/10.2147/DDDT.S499641

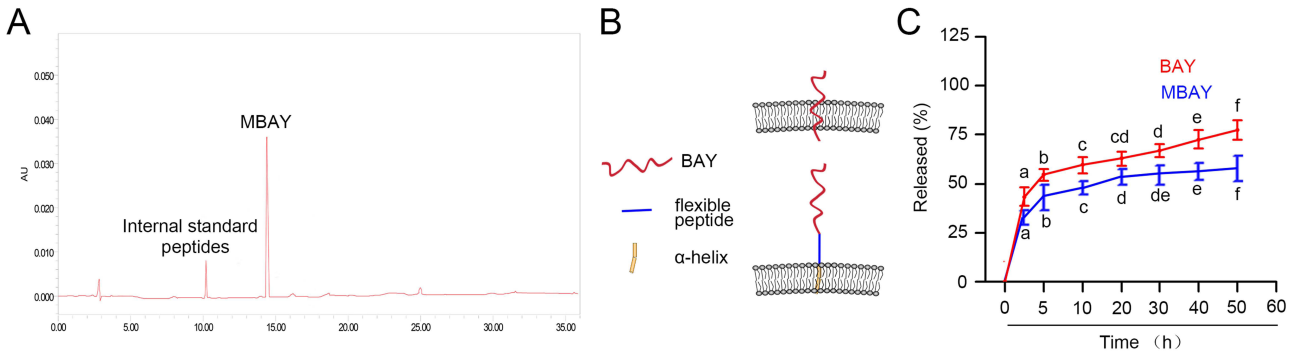

Figure 3 In vitro release profile of MBAY- exosome-SPION. (**A**) HPLC chromatogram of MBAY and internal standard peptide; (**B**) Schematic diagram of the sustained-release mechanism of MBAY (**C**) Release curve of BAY 55-9837 or MBAY loaded by exosome-SPION, their concentration was detected by HPLC. Multiple comparison analysis of data was performed for each experimental condition. Bars with same letter do not differ significantly. n = 6.

h. The results suggested that the employment of the α-helical structure significantly reduced the polypeptide release from the exosome. Moreover, using OriginPro 2021, the release kinetics analysis of BAY 55-9837 and MBAY was carried out, and the first - order fitted release equations were obtained. For BAY 55-9837, it is $y = 53.92 \times (1 - \exp(-0.17 \times x))$, and for MBAY, it is $y = 42.49 \times (1 - \exp(-0.12 \times x))$. From the above equations, it can be inferred that the release rate of MBAY is relatively slower. The reason for this is that the single transmembrane α-helix structure, due to its hydrophobic lipophilic nature, could hinder the polypeptide from leaking out of the exosome (Figure 3B).

Effects of MBAY-Exosome-SPION on β-Cell Functionality

Figure 4A revealed that both BAY 55-9837, BAY-exosome-SPION/MF, and MBAY-exosome-SPION/MF could significantly enhance insulin secretion compared to the model group.[28] VPAC II-mediated insulin secretion mainly occurs

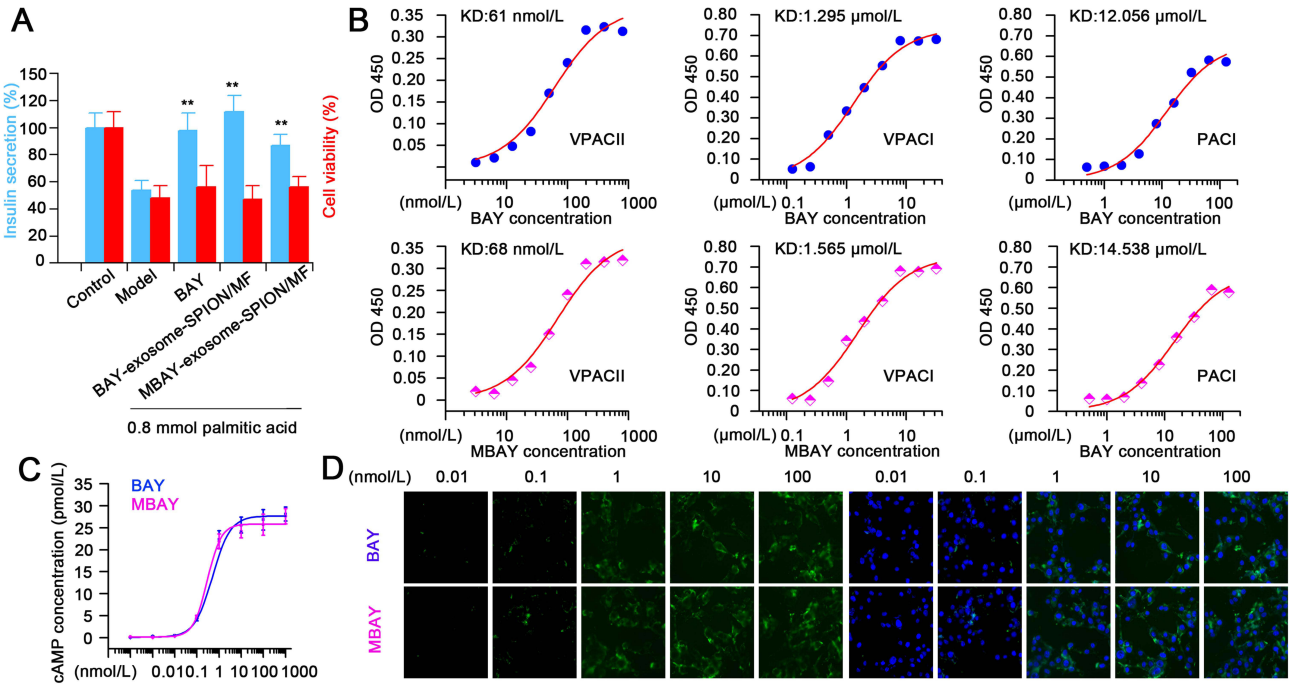

Figure 4 (**A**) The impacts of 100 nmol/L BAY 55-9837, BAY-exosome-SPION/MF, and MBAY-exosome-SPION/MF on insulin secretion or cell viability of MIN-6 cells in the presence of 8.3 mmol/L GLC and 0.8 mmol/L palmitic acid. The cell viability was detected by MTT and insulin concentration was detected by mouse insulin ELISA. (**B**) The binding affinity of BAY 55-9837 and MBAY with VPAC I, VPA II, and PAC1 was quantified by Originpro 2021 software according to the results of ELISA. (**C**) The effects of MBAY on cAMP content was detected by ELISA. (**D**) The effects of MBAY on Ca^{2+} in MIN-6 cells was measured by Ca^{2+} probe Fluo-3 AM. n = 6, significance levels are shown as $^{**}p < 0.01$ vs 0 control.

 https://doi.org/10.2147/DDDT.S499641

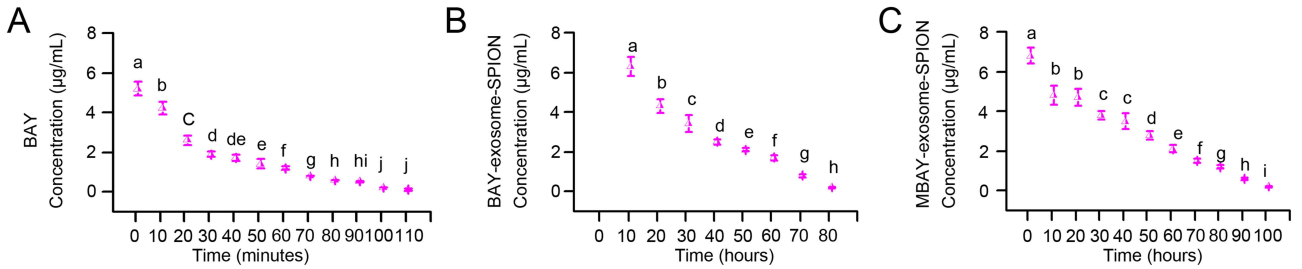

Figure 5 Plasma concentration-time curve of BAY 55-9837 in Kunming mice following the tail-vein injection of 5 mg/kg (**A**) BAY 55-9837, (**B**) BAY-exosome-SPION, or (**C**) MBAY-exosome-SPION. The concentration of BAY 55-9837 or MBAY was detect by HPLC. Multiple comparison analysis of data was performed for each experimental condition. Bars with same letter do not differ significantly. n = 6.

via the cAMP/PKA/Ca2+ signaling pathway.[29] The introduction of an α-helix in BAY 55-9837 may likely influence its affinity and specificity for the receptor as well as the associated signaling pathways. Hence, we analyzed the binding capacity of MABY to different receptors. In comparison to BAY 55-9837, MBAY still maintained high affinity and selectivity for VPAC II, and its Kd value is 68 nmol/L, while the affinity for the VPAC I and PACI receptors is relatively low, with Kd values of 1.565 μmol/L and 14.538 μmol/L, respectively (Figure 4B). Subsequently, we further examined the impact of MBAY on the VPAC II-mediated insulin secretion signaling pathway. The results of Figure 4C and D demonstrated that MBAY concentration-dependently increased the cAMP concentration and Ca^{2+} concentration in pancreatic islet cells. Therefore, it can be verified that the insulin secretion promoting signaling pathway of MBAY is consistent with that of BAY 55-9837. Both are mainly through the cAMP/PKA/Ca^{2+} signaling pathway.

In Vivo Pharmacokinetic Profile of MBAY-Exosome-SPION

The in vivo half-life of MBAY-exosome-SPION was further investigated in Kunming mice. The plasma concentration-time curve (Figures 5A–C) shows that BAY 55-9837 could not be detected at 110 min after injection. When BAY 55-9837 was loaded into exosome-SPION, it could still be detected at 80 h, and the MBAY within the exosome-SPION could still be detected at 100 h. Table 1 shows the relevant pharmacokinetic parameters of BAY 55-9837, BAY-exosome-SPION and MBAY-exosome-SPION. BAY 55-9837 had a high blood clearance rate of 29.9 mL/h and a short half-life of 0.37 h. However, when loaded into exosome-SPION, the blood clearance rate of BAY 55-9837 decreased to 0.488 mL/h, and the circulating half-life was prolonged to 9.45 h. he pharmacokinetic parameters of MBAY were further enhanced. Compared with BAY-exosome-SPION, the blood clearance rate of MBAY-exosome-SPION decreased to 0.343 mL/h and the half-life was prolonged to 18.02 h, with the in vivo half-life being prolonged by twice. Compared with BAY 55-9837, the in vivo blood clearance rate of BAY-exosome-SPION and MBAY-exosome-SPION is reduced, and the half-life is prolonged. This is because the exosome-based nano-delivery system can shield BAY55 - 9837 and MBAY from degradation or elimination by glomerular filtration. The improvement in the pharmacokinetic parameters of MBAY-

Table 1 Pharmacokinetic Parameters of MBAY-Exosome-SPION in Mouse Plasma

Parameters	BAY 55-9837 (Mean ± SD)	BAY-Exosome-SPION (Mean ± SD)	MBAY-Exosome-SPION (Mean ± SD)
Dose (μg/mL)	625	625	625
Total dose (μg)	125	125	125
$T_{1/2}$ (h)	0.37[a]	9.45[b]	18.02[C]
AUC_{0-t} (μg·h /mL)	4.175[a]	256.2[b]	364.5[C]
CL_{obs} (mL·h)	29.9[a]	0.488[b]	0.343[C]

Notes: Multiple comparison analysis of data was performed for each experimental condition. Results with the same letter do not differ significantly.

https://doi.org/10.2147/DDDT.S499641

exosome-SPION compared to BAY-exosome-SPION is attributed to the fusion of BAY 55-9837 with the a-helix, which enables a sustained release effect within the exosome.

Optimization the Administration Mode of MBAY-Exosome-SPION/MF

The L9(3^4) orthogonal design method was employed to optimize the drug administration mode. Three main factors, namely magnetic field intensity, drug concentration, and magnetic field action time, were set as variables. The time for the blood GLC value to decrease to the average fasting blood GLC value of T2DM mice (22 mmol/L) was taken as the investigation index. Based on these, an optimization experiment was carried out. A shorter time for the blood GLC value to decrease to the average fasting blood GLC value of T2DM mice indicates an optimal combined drug administration mode. Firstly, the value range intervals of the three factors were determined. Each factor was set at three levels, as shown in Table 2. Based on the above factors and levels, with the time for the blood GLC value to decrease to 22 mmol/L as the investigation index, a high-drug concentration experimental group (1.25, 2.5, and 5 mg/kg) and a low-concentration drug experimental group (0.25, 0.5, and 1 mg/kg) were set up. The experiment was conducted according to the orthogonal design L9(3^4) table, and the results are presented in Table 1. The range R was calculated using the intuitive analysis method. The left part of the table is the high-concentration experimental group, and the result shows that the range R value of the magnetic field action time is 0.24, which is greater than the range R value of the blank column 0.08. Therefore, within the high-concentration range, the magnetic field action time is the main factor affecting the restoration of blood GLC. The right portion of the table pertains to the low-concentration experimental group, and the scopes of the magnetic field intensity, drug concentration, and magnetic field action time are all larger than that of the blank column 0.09. Hence, within the low-concentration range, these three factors all exert an impact on the hypoglycemic effect of this drug, with drug concentration and time being the first two influential factors.

As depicted in Figure 6A and B, it visually shows the influence of each factor on the time needed for the blood GLC value to decrease to the average fasting blood GLC value of diabetic mice (22 mmol/L). The findings suggest that increasing the drug concentration, enhancing the magnetic field intensity, and prolonging the time can lead to the optimal drug administration effect.

Therapeutic Effect of MBAY-Exosome-SPION/MF in Vivo

To explore the long-term therapeutic efficacy of MBAY-exosome-SPIONs/MF, T2DM model mice were intravenously injected with BAY 55-9837, BAY-exosome-SPIONs/MF, and MBAY-exosome-SPIONs/MF for 8 weeks. Weight gain is a typical sign of T2DM. Therefore, the body weights of the T2DM mice were measured. The findings revealed that the body weights of the mice in the BAY 55-9837 and BAY-exosome-SPIONs treatment groups were decreased compared to those in the T2DM model group mice. Further reduction in body weight was noted in the T2DM model mice treated with MBAY-exosome-SPIONs/MF when compared with those treated with BAY 55-9837 and BAY-exosome-SPIONs/MF (Figure 7A).

The increase in TG level is the core defect in abnormal lipid metabolism related to diabetes. These lipid changes associated with diabetes are typically attributed to the elevated concentration of free fatty acids due to insulin resistance.[30] Hence, the blood TG of the T2DM mice was measured. MBAY-exosome-SPIONs/MF showed the best therapeutic effects in reducing blood TG in T2DM model mice compared to BAY 55-9837 and BAY-exosome-SPIONs /MF, indicating that it has a better ability to improve lipid metabolism (Figure 7B).

The liver is highly involved in regulating blood GLC levels, and liver function disorders often occur in T2DM.[31] As shown in Figure 7C and D, MBAY-exosome-SPIONs/MF showed the most excellent therapeutic efficacy in reducing hepatic glycogen and hepatic TG in T2DM model mice compared with BAY 55-9837 and BAY-exosome-SPIONs, indicating that it has a superior ability to enhance liver function.

Glycosylated hemoglobin is the gold standard for blood GLC assessment and is widely used in the clinic.[32] Figure 7E shows that the daily administration of MBAY-exosome-SPIONs/MF in T2DM model mice had the greatest ability to reduce glycosylated hemoglobin (by 14%) compared with BAY 55-9837 and BAY-exosome-SPION/MF, further confirming that the sustained-release capacity of MBAY in the exosome can significantly improve the therapeutic effect in treating T2DM.

Table 2 L9(3^4) Orthogonal Array for Optimization of MBAY-Exosome-SPION/MF Administration Mode

	Column NO.	**1(T)**	**2 (mg/kg)**	**3 (h)**	**4**	**Time (h)**		**Column NO.**	**1(T)**	**2 (mg/kg)**	**3 (h)**	**4**	**Time (h)**
	Factor	A (MF)	B(Concentration)	C (Time)				Factor	A (MF)	B(Concentration)	C (Time)		
Test No.	1	1 (1)	1 (1.25)	1 (0.5)	1	1.78	Test No.	1	1 (1)	1 (0.25)	1 (0.5)	1	2.08
	2	1	2 (2.5)	2 (1)	2	1.61		2	1	2 (0.5)	2 (1)	2	1.81
	3	1	3 (5)	3 (2)	3	1.53		3	1	3 (1)	3 (2)	3	1.71
	4	2 (2)	1	2	3	1.69		4	2 (2)	1	2	3	1.99
	5	2	2	3	1	1.48		5	2	2	3	1	1.65
	6	2	3	1	2	1.67		6	2	3	1	2	1.77
	7	3 (3)	1	3	2	1.45		7	3 (3)	1	3	2	1.71
	8	3	2	1	3	1.74		8	3	2	1	3	1.85
	9	3	3	2	1	1.61		9	3	3	2	1	1.66
	K1	4.92	4.92	5.19	4.87			K1	5.60	5.78	5.7	5.39	
	K2	4.84	4.83	4.91	4.73			K2	5.41	5.31	5.46	5.29	
	K3	4.8	4.81	4.46	4.96			K3	5.22	5.14	5.07	5.55	
	$\overline{K1}$	1.64	1.64	1.73	1.62			$\overline{K1}$	1.87	1.93	1.9	1.80	
	$\overline{K2}$	1.61	1.61	1.64	1.58			$\overline{K2}$	1.80	1.77	1.82	1.76	
	$\overline{K3}$	1.60	1.60	1.49	1.65			$\overline{K3}$	1.74	1.71	1.69	1.85	
	R	0.04	0.04	0.24	0.08			R	0.127	0.217	0.21	0.09	
Optimum factor combination A3B3C3 (3 T, 5 mg/kg, 2 h)								Optimum factor combination A3B3C3(3 T, 1 mg/kg, 2 h)					

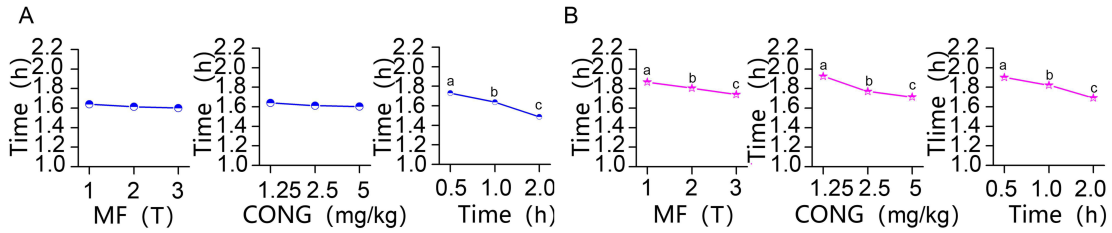

Figure 6 Orthogonal analysis of drug administration mode according to Table 2. (**A**) MF, concentration, and the used MF time on time for the blood GLC value to decrease to the average fasting blood GLC value of T2DM mice (22 mmol/L) in high concentration group. (**B**) MF, concentration, and the used MF time on time for the blood GLC value to decrease to the average fasting blood GLC value of T2DM mice (22 mmol/L) in low concentration group. Multiple comparison analysis of data was performed for each experimental condition. Bars with same letter do not differ significantly. n = 6.

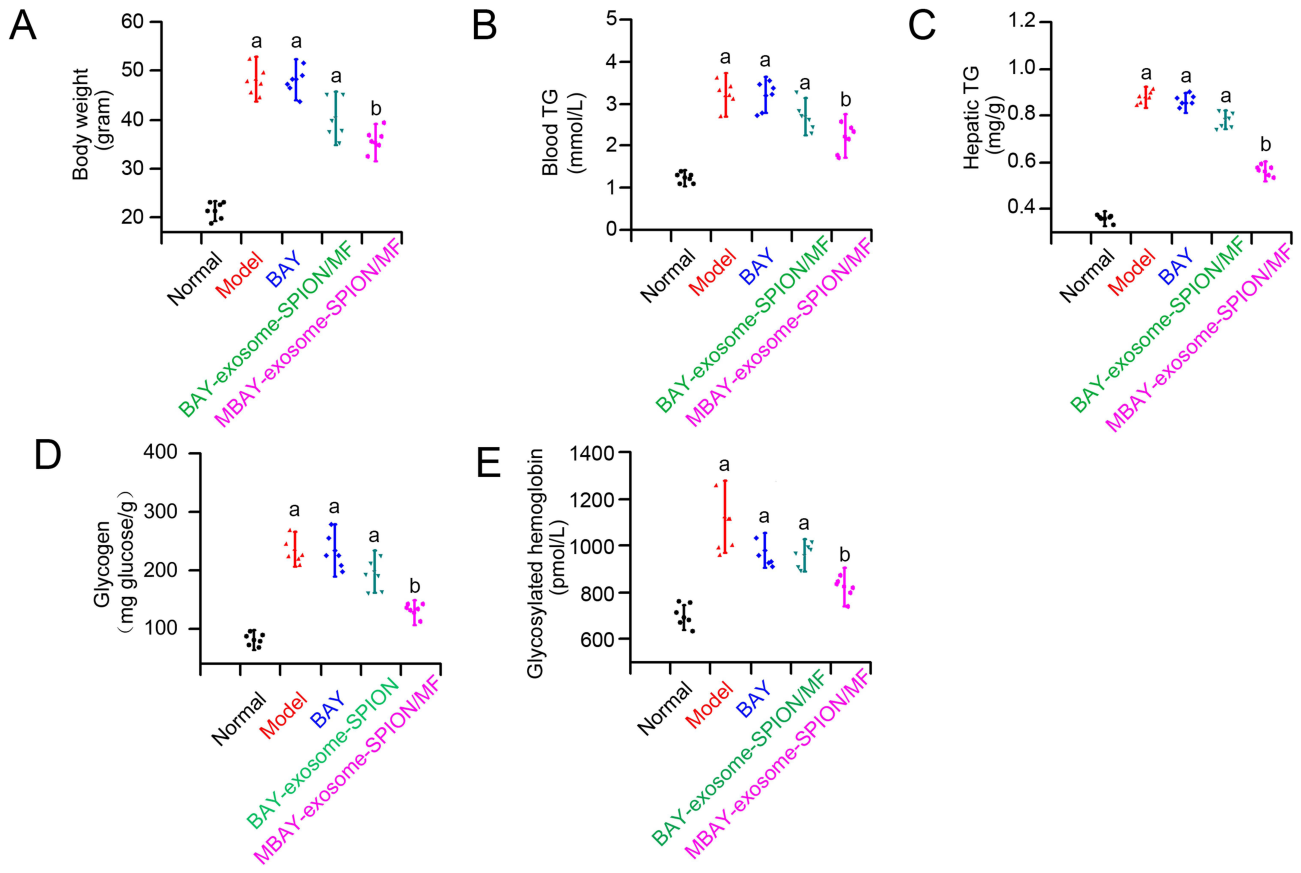

Figure 7 Chronic therapeutic effects of MBAY-exosome-SPIONs/MF on T2DM model mice. Effect of MBAY-exosome-SPIONs/MF on (**A**) body weight, (**B**) blood TG, (**C**) hepatic TG, (**D**) hepatic glycogen, and (**E**) glycosylated hemoglobin. Glycosylated hemoglobin was determined using ELISA Kit (BMASSAY, Beijing, China). The TG level was measured with a Triglyceride Quantification Kit. And the hepatic glycogen level was measured with a Glycogen Content Kit. Multiple comparison analysis of data was performed for each experimental condition. Bars with same letter do not differ significantly. n = 6.

Discussion

Achieving GLC control is a crucial strategy in the treatment of T2DM.[33] Currently, the treatment of T2DM mainly relies on several strategies aimed at reducing hyperglycemia. However, the majority of these therapeutics cannot sense and respond appropriately to the increase in blood GLC, thus showing limited therapeutic effectiveness. Insulin injection is the most important therapeutic method in the treatment of diabetes mellitus and its complications[34,35] Nevertheless, if the dosage of insulin is not precisely controlled, it may cause life-threatening hypoglycemia.[36] Oral hypoglycemic agents, such as metformin and sulfonylureas, play crucial roles in managing blood glucose levels. Importantly, these hypoglycemic drugs have adverse effects according to the mechanism of blood glucose regulation. These include gastrointestinal

tract reactions, hypoglycemia, low white blood cell count, hemolytic anemia, an increased risk of major cardiovascular events, and weight gain. BAY 55-9837, a highly selective VPAC II agonist, has the ability to potentiate insulin secretion in response to elevated blood GLC and is regarded as a potential peptide therapeutic agent for T2DM.[12]

Blood GLC can be effectively controlled by increasing the drug concentration in pancreatic tissues, thereby enhancing its GLC responsiveness frequency. However, the promising therapeutic effect of BAY 55-9837 is limited by its extremely short half - life, resulting in a limited blood glucose responsiveness. Our previous study has shown that SPION-exosome has a high drug loading efficiency for BAY 55-9837.[17] Meanwhile, the protective effect of exosomes gives BAY 55-9837 a longer plasma half - life, and the active targeting property of SIPONs allows BAY - exosomes to obtain a favorable targeting ability. Unfortunately, exosomes have a common drawback: an initial uncontrolled burst release of the drug.[36] Due to the certain fluidity of the exosome structure at body temperature, the release pores of exosomes cannot be regulated.[16] BAY 55-9837 is a polypeptide, which can be reconstructed through genetic engineering to obtain a fusion protein that increases its hydrophobicity, thereby achieving the sustained release ability from exosomes. In this study, the α-helical hydrophobic peptide segment within CD81, the exosomal marker protein, was successfully fused with BAY 55-9837 to obtain MBAY F1, MBAY F2, MBAY F3, and MBAY F4. The transmembrane domain of CD81 is distributed on the surface of exosomes, and its sequence and crystal structure have been fully determined.[23] The results indicated that MBAY F1 fused with one alpha helix maintained the same insulin secretion-promoting ability as BAY 55-9837. Meanwhile, the affinity analysis and signal pathway verification further confirmed that the reconstructed MBAY F1 still retained high affinity with VPAC II rather than VPAC I and PAC1, and could activate the VPAC II-mediated signal pathway by increasing the cAMP concentration and Ca^{2+} concentration.

The combination of diabetology and nanotechnology shows great promise and has the potential to transform the management and treatment of diabetes mellitus. Nanotechnology-based controlled drug delivery systems are regarded as a potential approach for therapeutic protein delivery.[37] Our results demonstrated that MBAY F1 was successfully loaded into exosome-SPION to gain MBAY-exosome-SPION. Our results showed that MBAY F1 was successfully incorporated into exosome-SPION to obtain MBAY-exosome-SPION. The morphological and size results revealed that MBAY-exosome-SPIONs were successfully produced and collected through MF, having a uniform size and shape with an approximate diameter. Furthermore, it was observed that the SPIONs were clearly distributed on the surface of the exosomes.

SPION-exosome can be guided to the target location with the help of an external MF. This facilitates the clinical translation and application of targeted drug delivery.[38] For polypeptide diabetes drugs, sustained release and increasing the half-life are important directions in new drug development.[39] The targeted carrier can stabilize the drug concentration in the pancreatic region for a relatively long time. Moreover, the operation of applying an external MF to pancreatic islets is simple and convenient. Magnetic targeting is more likely to be effective in regions with a slower blood flow.[18,40] Furthermore, mature pancreatic islets are highly vascularized by a dense capillary network, and the blood flow in pancreatic tissue is significantly reduced in T2DM patients.[41,42]

An ideal sustained protein/peptide delivery system should meet the following requirements to achieve long-term treatment of chronic diseases with minimized dosage and frequency: (1) provide high loading efficiency of the targeted therapeutics; (2) protect the loaded therapeutics from degradation; and (3) regulate drug release to maintain a steady-state concentration for an extended period in the target tissues or organs.[43] Exosomes consist of natural lipid bilayers. Therefore, the α-helix structure within MBAY can easily interact with exosome membranes, subsequently reducing its release and thereby playing a blocking role to retard the release of MBAY from exosomes. The in vitro and in vivo release profiles demonstrated that compared with BAY-exosome-SPION, the release rate of MBAY was more stable without the occurrence of initial burst release. Meanwhile, pancreatic magnetic targeting technology was employed for optimal GLC control. Thus, in combination with the application of exosome-SPION/MF, MBAY-exosome-SPION/MF fulfilled all the conditions that an ideal sustained protein/peptide delivery system should possess.

Additionally, there are multiple variables in the application of MBAY-exosome-SPION/MF when treating T2DM. Hence, the L9(3^4) orthogonal design method was adopted to optimize the drug administration modality. Via the orthogonal experiment, the impact of diverse factors on blood GLC can be observed and quantified.[44] Subsequently, the optimal combination of factors can be determined to enhance the effect of MBAY-exosome-SPION/MF on GLC

control. The results showed that increasing the drug concentration, enhancing the magnetic field intensity, and prolonging the time led to the optimal hypoglycemic effect of MBAY-exosome-SPION/MF. The effects of MBAY-exosome-SPION /MF on the insulin secretagogue capacity were also validated in vivo. Long-term experimental data indicated that the treatment with MBAY-exosome-SPION/MF (with a density of 3 T, for 1 h, twice a day) significantly improved T2DM symptoms such as body weight, glycosylated hemoglobin, plasma triglycerides, and hepatic triglycerides, thereby suggesting the potential application of MBAY-exosome-SPION/MF.

Conclusion

The α-helical hydrophobic peptide segment of the exosomal marker protein CD81 was fused with BAY 55-9837 to create MBAY F1, which was then loaded into exosome-SPION/MF to address the initial burst release problem of the exosome-SPION drug. The α-helical hydrophobic peptide segment in MBAY F1 enabled the slow and sustained release of the drug from the exosome-SPION. The exosome's protective effect and the active targeting property of SPION/MF endow MBAY F1 with a longer half-life and an ideal targeting capability. By achieving sustained drug release, this can effectively improve the compliance in diabetes treatment and enhance the therapeutic effect. By endowing the insulinotropic drug with targeted performance, it can maintain a long-term and stable drug concentration at the target site of pancreatic β cells. This leads to a better realization of the blood glucose response and the achievement of long-term treatment. Therefore, our research has demonstrated that in the treatment of T2DM, targeting exosomes as drug carriers and sustained-release modified polypeptides can significantly improve the patient's compliance and control blood sugar, possessing remarkable clinical and application values.

Abbreviations

CS, chitosan; GLC, glucose; huMSC, human mesenchymal stem cell; HPLC, high-performance liquid chromatography; HFD, high-fat diet; MF, magnetic force; MTT, 3-(4,5-dimethyl-2-thiazolyl)-2,5-diphenyl-2-H-tetrazolium bromide; NHS, N-hydroxysuccinimidyl; PAC1, Pituitary adenylate cyclase-activating polypeptide type 1 receptor; PBS, phosphate buffered saline; PBST, Phosphate Buffered Saline with Tween-20; SPION, superparamagnetic iron oxide nanoparticle; STZ, streptozocin; T2DM, type 2 diabetes mellitus; TEM, transmission electron microscopy; VPAC II,vasoactive intestinal peptide receptor type 2; VPAC I, vasoactive intestinal peptide receptor type 1.

Funding

This work was supported by Guangdong Basic and Applied Basic Research Foundation (number 2020A1515110862 and 2021B1515140060), Youth Fund of the National Natural Science Foundation of China (number 82204435), Special Project for Clinical and Basic Sci&Tech Innovation of Guangdong Medical University(number GDMULCJC2024168) and Shaoguan College students' innovation and entrepreneurship training program (number Sycxcy2024190).

Disclosure

The author(s) report no conflicts of interest in this work.

References

1. Ahmad E, Lim S, Lamptey R, et al. Type 2 diabetes. *Lancet*. 2022;400(10365):1803–1820. doi:10.1016/s0140-6736(22)01655-5
2. Demir S, Nawroth PP, Herzig S, et al. Emerging targets in type 2 diabetes and diabetic complications. *Adv Sci*. 2021;8(18):e2100275. doi:10.1002/advs.202100275
3. Bowering K, Case C, Harvey J, et al. Faster aspart versus insulin aspart as part of a basal-bolus regimen in inadequately controlled type 2 diabetes: the onset 2 trial. *Diabetes Care*. 2017;40(7):951–957. doi:10.2337/dc16-1770
4. Lee Y-M, Ha C-M, Kim S-A, et al. Low-dose persistent organic pollutants impair insulin secretory function of pancreatic β-cells: human and *in vitro* evidence. *Diabetes*. 2017;66(10):2669–2680. doi:10.2337/db17-0188
5. Artasensi A, Pedretti A, Vistoli G, et al. Type 2 diabetes mellitus: a review of multi-target drugs. *Molecules*. 2020;25(8):1987. doi:10.3390/molecules25081987
6. Haahr H, Fita EG, Heise T. A review of insulin degludec/insulin aspart: pharmacokinetic and pharmacodynamic properties and their implications in clinical use. *Clin Pharmacokinet*. 2017;56(4):339–354. doi:10.1007/s40262-016-0455-7
7. Bue-Valleskey JM, Kazda CM, Ma C, et al. Once-weekly basal insulin fc demonstrated similar glycemic control to once-daily insulin degludec in insulin-naive patients with type 2 diabetes: a Phase 2 randomized control trial. *Diabetes Care*. 2023;46(5):1060–1067. doi:10.2337/dc22-2396

8. Lv W, Wang X, Xu Q, et al. Mechanisms and characteristics of sulfonylureas and glinides. *Curr Top Med Chem*. 2020;20(1):37–56. doi:10.2174/1568026620666191224141617
9. Nathan DM, Lachin JM, Balasubramanyam A, et al. Glycemia reduction in type 2 diabetes - glycemic outcomes. *N Engl J Med*. 2022;387(12):1063–1074. doi:10.1056/NEJMoa2200433
10. Heise T. Novel drugs for diabetes therapy. *Handb Exp Pharmacol*. 2022;274:415–438. doi:10.1007/164_2021_574
11. Lim S, Kim KM, Nauck MA. Glucagon-like peptide-1 receptor agonists and cardiovascular events: class effects versus individual patterns. *Trends Endocrinol Metab*. 2018;29(4):238–248. doi:10.1016/j.tem.2018.01.011
12. Pan CQ, Li F, Tom I, et al. Engineering novel vpac2-selective agonists with improved stability and glucose-lowering activity *in vivo*. *J Pharmacol Exp Ther*. 2007;320(2):900–906. doi:10.1124/jpet.106.112276
13. Bertrand G, Puech R, Maisonnasse Y, et al. Comparative effects of pacap and vip on pancreatic endocrine secretions and vascular resistance in rat. *Br J Pharmacol*. 1996;117(4):764–770. doi:10.1111/j.1476-5381.1996.tb15256.x
14. Sharma DK, Pattnaik G, Behera A. Recent developments in nanoparticles for the treatment of diabetes. *J Drug Targeting*. 2023;31(9):908–919. doi:10.1080/1061186X.2023.2261077
15. Kalluri R, LeBleu VS. The biology, function, and biomedical applications of exosomes. *Science*. 2020;367(6478):6977. doi:10.1126/science.aau6977
16. Lai RC, Yeo RW, Tan KH, et al. Exosomes for drug delivery - a novel application for the mesenchymal stem cell. *Biotechnol Adv*. 2013;31(5):543–551. doi:10.1016/j.biotechadv.2012.08.008
17. Zhuang M, Du D, Pu L, et al. Spion-decorated exosome delivered bay55-9837 targeting the pancreas through magnetism to improve the blood glc response. *Small*. 2019;15(52):e1903135. doi:10.1002/smll.201903135
18. Qi H, Liu C, Long L, et al. Blood exosomes endowed with magnetic and targeting properties for cancer therapy. *ACS Nano*. 2016;10(3):3323–3333. doi:10.1021/acsnano.5b06939
19. Tian Y, Li S, Song J, et al. A doxorubicin delivery platform using engineered natural membrane vesicle exosomes for targeted tumor therapy. *Biomaterials*. 2014;35(7):2383–2390. doi:10.1016/j.biomaterials.2013.11.083
20. Wei H, Hu Y, Wang J, et al. Superparamagnetic iron oxide nanoparticles: cytotoxicity, metabolism, and cellular behavior in biomedicine applications. *Int J Nanomed*. 2021;16:6097–6113. doi:10.2147/ijn.S321984
21. Sharma DK. Recent advances in medical applications of chitosan-based biomaterials. *Int J Polym Mater Polym Biomater*. 2024;2024:1–16. doi:10.1080/00914037.2024.2391345
22. Salunkhe S, Dheeraj, Basak M, et al. Surface functionalization of exosomes for target-specific delivery and *in vivo* imaging & tracking: strategies and significance. *J Control Release*. 2020;326:599–614. doi:10.1016/j.jconrel.2020.07.042
23. Alvarez KG, Goral L, Suwandi A, et al. Human tetraspanin CD81 facilitates invasion of Salmonella enterica into human epithelial cells. *Virulence*. 2024;15(1):2399792. doi:10.1080/21505594.2024.2399792
24. Morais LM, Chaves TS, Medeiros MA, et al. Selection and characterization of single-stranded DNA aptamers of diagnostic potential against the whole zika virus. *Viruses*. 2022;14(9):1867. doi:10.3390/v14091867
25. Rao L, Ma Y, Zhuang M, et al. Chitosan-decorated selenium nanoparticles as protein carriers to improve the *in vivo* half-life of the peptide therapeutic BAY 55-9837 for type 2 diabetes mellitus. *Int J Nanomed*. 2014;9:4819–4828. doi:10.2147/ijn.S67871
26. Perugini V, Best M, Kumar S, et al. Carboxybetaine-modified succinylated chitosan-based beads encourage pancreatic β-cells (min-6) to form islet-like spheroids under *in vitro* conditions. *J Mater Sci Mater Med*. 2017;29(1):15. doi:10.1007/s10856-017-6018-0
27. Cheng Y, Yu X, Zhang J, et al. Pancreatic kallikrein protects against diabetic retinopathy in kk cg-a(y)/j and high-fat diet/streptozotocin-induced mouse models of type 2 diabetes. *Diabetologia*. 2019;62(6):1074–1086. doi:10.1007/s00125-019-4838-9
28. Mazzocchi G, Malendowicz LK, Neri G, et al. Pituitary adenylate cyclase-activating polypeptide and pacap receptor expression and function in the rat adrenal gland. *Int J mol Med*. 2002;9(3):233–243.
29. Giordanetto F, Revell JD, Knerr L, et al. Stapled vasoactive intestinal peptide (vip) derivatives improve vpac2 agonism and glucose-dependent insulin secretion. *ACS Med Chem Lett*. 2013;4(12):1163–1168. doi:10.1021/ml400257h
30. Poznyak A, Grechko AV, Poggio P, et al. The diabetes mellitus-atherosclerosis connection: the role of lipid and glucose metabolism and chronic inflammation. *Int J mol Sci*. 2020;21(5):1835. doi:10.3390/ijms21051835
31. Gastaldelli A, Stefan N, Häring HU. Liver-targeting drugs and their effect on blood glucose and hepatic lipids. *Diabetologia*. 2021;64(7):1461–1479. doi:10.1007/s00125-021-05442-2
32. Lee J, Cho JH. Early glycosylated hemoglobin target achievement predicts clinical outcomes in patients with newly diagnosed type 2 diabetes mellitus. *Diabetes Metab J*. 2021;45(3):337–338. doi:10.4093/dmj.2021.0078
33. Almomani MH, Al-Tawalbeh S. Glycemic control and its relationship with diabetes self-care behaviors among patients with type 2 diabetes in northern Jordan: a cross-sectional study. *Patient Prefer Adherence*. 2022;16:449–465. doi:10.2147/ppa.S343214
34. Roumie CL, Hung AM, Greevy RA, et al. Comparative effectiveness of sulfonylurea and metformin monotherapy on cardiovascular events in type 2 diabetes mellitus: a cohort study. *Ann Intern Med*. 2012;157(9):601–610. doi:10.7326/0003-4819-157-9-201211060-00003
35. DePeralta DK, Wei L, Ghoshal S, et al. Metformin prevents hepatocellular carcinoma development by suppressing hepatic progenitor cell activation in a rat model of cirrhosis. *Cancer*. 2016;122(8):1216–1227. doi:10.1002/cncr.29912
36. Bakadia BM, Qaed Ahmed AA, Lamboni L, et al. Engineering homologous platelet-rich plasma, platelet-rich plasma-derived exosomes, and mesenchymal stem cell-derived exosomes-based dual-crosslinked hydrogels as bioactive diabetic wound dressings. *Bioact Mater*. 2023;28:74–94. doi:10.1016/j.bioactmat.2023.05.002
37. Karwasra R, Sharma S, Sharma I, et al. Diabetology and nanotechnology: a compelling combination. *Recent Pat Nanotechnol*. 2023;19:4–16. doi:10.2174/0118722105253055231016155618
38. Wahajuddin W. Superparamagnetic iron oxide nanoparticles: magnetic nanoplatforms as drug carriers. *Int J Nanomed*. 2012;7:3445–3471. doi:10.2147/ijn.S30320
39. Nguyen TTK, Pham K-Y, Yook S. Engineered therapeutic proteins for sustained-release drug delivery systems. *Acta Biomater*. 2023;171:131–154. doi:10.1016/j.actbio.2023.09.018
40. Cherry EM, Maxim PG, Eaton JK. Particle size, magnetic field, and blood velocity effects on particle retention in magnetic drug targeting. *Med Phys*. 2010;37(1):175–182. doi:10.1118/1.3271344

41. Bock T, Pakkenberg B, Buschard K. Genetic background determines the size and structure of the endocrine pancreas. *Diabetes*. 2005;54 (1):133–137. doi:10.2337/diabetes.54.1.133
42. Ballian N, Brunicardi FC. Islet vasculature as a regulator of endocrine pancreas function. *World J Surg*. 2007;31(4):705–714. doi:10.1007/s00268-006-0719-8
43. Nie TQ, Wang W, Liu XH, et al. Sustained release systems for delivery of therapeutic peptide/protein. *Biomacromolecules*. 2021;22(6):2299–2324. doi:10.1021/acs.biomac.1c00160
44. Zhang Y-L, Zhang K-Y, Zhu Z-C. Optimal design of impeller for self-priming pump based on orthogonal method. *Sci Rep*. 2023;13(1):16491. doi:10.1038/s41598-023-43663-0